

Two dimensional polymer-embedded quasi-distributed FBG pressure sensor for biomedical applications

George T. Kanellos^{1,3}, George Papaioannou,² Dimitris Tsiokos^{2,3}, Christos Mitrogiannis², George Nianos² and Nikos Pleros^{1,3}

¹ Department of Informatics, Aristotle University of Thessaloniki, Thessaloniki, Greece

² MOVE Center, College of Engineering and Applied Science, Wisconsin Institute for Biomedical Health Technology, University of Wisconsin Milwaukee, Milwaukee, WI, USA

³ Centre for Research and Technology Hellas, Thessaloniki, Greece

*kanellos@csd.auth.gr

Abstract: We report on the development of a flexible 2D optical fiber-based pressure sensing surface suitable for biomedical applications. The sensor comprises of highly-sensitive Fiber Bragg Grating elements embedded in a thin polymer sheet to form a 2x2 cm² sensing pad with a minimal thickness of 2.5mm, while it is easily expandable in order to be used as a building block for larger surface sensors. The fabricated pad sensor was combined with a low physical dimension commercially available interrogation unit to enhance the portability features of the complete sensing system. Sensor mechanical properties allow for matching human skin behavior, while its operational performance exhibited a maximum fractional pressure sensitivity of 12 MPa⁻¹ with a spatial resolution of 1x1cm² and demonstrated no hysteresis and real time operation. These attractive operational and mechanical properties meet the requirements of various biomedical applications with respect to human skin pressure measurements, including amputee sockets, shoe sensors, wearable sensors, wheelchair seating-system sensors, hospital-bed monitoring sensors.

©2009 Optical Society of America

OCIS codes: (170.1470) Blood or tissue constituent monitoring; (230.0230) Optical devices.

References and links

1. C. Bansal, R. Scott, D. Stewart, and C. J. Cockerell, "Decubitus ulcers: a review of the literature," *Int. J. Dermatol.* **44**(10), 805–810 (2005).
2. A. A. Polliack, R. C. Sieh, D. D. Craig, S. Landsberger, D. R. McNeil, and E. Ayyappa, "Scientific validation of two commercial pressure sensor systems for prosthetic socket fit," *Prosthet. Orthot. Int.* **24**(1), 63–73 (2000).
3. C. Pramanik, H. Saha, and U. Gangopadhyay, "Design optimization of a high performance silicon MEMS piezoresistive pressure sensor for biomedical applications," *J. Micromech. Microeng.* **16**(10), 2060–2066 (2006).
4. A. Othonos, and K. Kalli, *Fiber Bragg Gratings: Fundamentals and Applications in Telecommunications and Sensing*. Boston, MA: Artech, 1999, ISBN 0–89006–344–3.
5. W. W. Morey, G. Meltz, and W. H. Glenn, "Fiber optic Bragg grating sensors," in *Proc. SPIE, Fiber Optics and Laser Sensors VII*, vol. 1169, 1989.
6. A. D. Kersey, M. A. Davis, H. J. Patrick, M. LeBlanc, K. P. Koo, C. G. Askins, M. A. Putnam, and E. J. Friebele, "Fiber grating sensors," *J. Lightwave Technol.* **15**(8), 1442–1463 (1997).
7. H. J. Sheng, M.-Y. Fu, T.-C. Chen, W.-F. Liu, and S.-S. Bor, "A lateral pressure sensor using a fiber Bragg grating," *IEEE Photon. Technol. Lett.* **16**(4), 1146–1148 (2004).
8. Y. Zhang, D. Feng, Z. Liu, Z. Guo, X. Dong, K. S. Chiang, and B. C. B. Chu, "High-sensitivity pressure sensor using a shielded polymer-coated fiber Bragg grating," *IEEE Photon. Technol. Lett.* **13**(6), 618–619 (2001).
9. T. Geernaert, G. Luyckx, E. Voet, T. Nasilowski, K. Chah, M. Becker, H. Bartelt, W. Urbanczyk, J. Wojcik, W. De Waele, J. Degrieck, H. Terryn, F. Berghmans, and H. Thienpont, "Transversal Load Sensing with Fiber Bragg Gratings in Microstructured Optical Fibers," *IEEE Photon. Technol. Lett.* **21**(1), 6–8 (2009).
10. M. A. Davis, D. G. Bellemore, M. A. Putnam, and A. D. Kersey, "Interrogation of 60 Fibre Bragg Grating Sensors with Microstrain Resolution Capability," *Electron. Lett.* **32**(15), 1393–1394 (1996).
11. S. C. Tjin, Y. Wang, X. Sun, P. Moyo, and J. M. W. Brownjohn, "Application of quasi-distributed fibre Bragg grating sensors in reinforced concrete structures," *Meas. Sci. Technol.* **13**(4), 583–589 (2002).

12. W. Du, X. M. Tao, H. Y. Tam, and C. L. Choy, "Fundamentals and applications of optical fiber Bragg grating sensors to textile structural composites," *Compos. Struct.* **42**(3), 217–229 (1998).
 13. J. W. Arkwright, N. G. Blenman, I. D. Underhill, S. A. Maunder, M. M. Szczesniak, P. G. Dinning, and I. J. Cook, "In-vivo demonstration of a high resolution optical fiber manometry catheter for diagnosis of gastrointestinal motility disorders," *Opt. Express* **17**(6), 4500–4508 (2009).
 14. C.-Y. Huang, W.-C. Wang, W.-J. Wu, and W. R. Ledoux, "Composite Optical Bend Loss Sensor for Pressure and Shear Measurement," *IEEE Sens. J.* **7**(11), 1554–1565 (2007).
 15. Francis Berghmans, "Photonic skins for optical sensing: highlights of the PHOSPHOS project", in *Optical Fiber Sensor Conference - OFS-20, Technical Digest (CD)* (Optical Society of America, 2009), paper OF101 08.
 16. <http://www.ibsen.dk/products/im/I-MON-80D-Interrogation-monitor>
 17. C. Jewart, K. P. Chen, B. McMillen, M. M. Bails, S. P. Levitan, J. Canning, and I. V. Avdeev, "Sensitivity enhancement of fiber Bragg gratings to transverse stress by using microstructural fibers," *Opt. Lett.* **31**(15), 2260–2262 (2006).
-

1. Introduction

Accurate, non-invasive and long-term monitoring of essential life parameters such as respiration, cardiac activity, blood pressure as well as the detection of skin stresses and contact pressure at the amputee socket-stump interface can improve significantly the prognostic, diagnostic and therapeutic efficiency of clinical decision making. Conventional human skin pressure measurement methods are classified based on their operation principle as fluid-filled sensors, pneumatic sensors, diaphragm deflection strain gauge, cantilever/beam strain gauge and printed circuit sheet sensors [1]. These sensors however possess many disadvantages in terms of reduced sensitivity, increased hysteresis, signal drift and low spatial resolution [1–3].

The rapidly evolving field of optical fiber sensing holds great potential for providing effective solutions towards accurately measuring and monitoring contact skin pressure, strain and shear at the human-machine interfaces. Sensing by means of light offers a number of advantages since light propagation is highly sensitive to external forces and can allow assessment of perturbations yielding real-time measurements with almost negligible hysteresis [4]. In addition, optical fibre sensors provide immunity to electromagnetic interference, high sensitivity, small size and low weight, passiveness, resistance to harsh environments, multiplexing capabilities and possibility to parallelize the readout [5]. Fiber Bragg Grating technology offers enhanced sensitivity [6–9] while its WDM interrogation method allows for multiplexing single element FBG sensors in arrays within a single fiber to form 1-D multipoint quasi-distributed sensing systems [10]. FBG quasi-distributed sensors have already found extensive application in civil engineering, automotive and aerospace for structural health monitoring [11,12].

However, limited work has been done in the field of healthcare towards synergizing photonic sensing with biomechanics, orthopaedics and rehabilitation applications. Within these attempts, a FBG-based pressure sensor has been demonstrated in the design of a high-resolution optical fiber manometry catheter [13]. On the other hand, fiber optic surface sensing structures for health-care pressure measurements have not yet been adequately addressed. To this end, a 2D fiber-sensing configuration was presented by Chu-Yu Huang et al. [14], where a 2D mesh of simple optical fibers embedded in a silicon-polymer material was used to assess shoe insole pressure, exhibiting however low sensitivity. Efforts in fabricating a 2D fiber sensing configuration with increased sensitivity are also currently being deployed in [15].

In this article, we report on the development of a 2D optical FBG-based pressure sensing surface that combines the advantages of the FBG-array sensors with novel, elastic and flexible Polydimethyl-siloxane (PDMS) polymer material to provide a light-weight, compliant and flexible 2D pressure sensing surface. The sensor comprises of highly-sensitive Fiber Bragg Grating elements embedded in a thin polymer sheet to form a 2x2 cm² sensing pad with a minimal thickness of 2.5mm, while it is easily expandable in order to be used as a building block for larger scale sensors. The sensor's enhanced performance exhibited a maximum fractional pressure sensitivity of 12 MPa⁻¹ with a spatial resolution of 1x1cm² while it

demonstrated no hysteresis and real time operation. The mechanical properties of this pad sensor makes it very unobtrusive while they allow for wrapping, embedding or attaching the

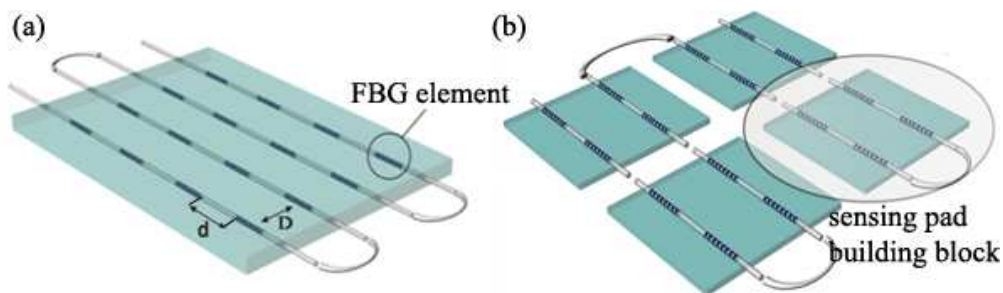


Fig. 1. a) PDMS 2D sensing surface with FBG-array optical sensing elements b) elementary 2D sensors used as building blocks for large scale surface sensors

sensor to irregular shapes and geometries, offering enhanced response to curvature. The fabricated pad sensor was combined with a low physical dimension commercially available interrogation unit [16] to enhance the portability features of the complete sensing system. The physical and operational characteristics of the presented pad sensor and particularly its high sensitivity in low absolute pressure values, its high spatial resolution and unobtrusive characteristics combined with potential portability are ideally suited for biomedical applications including amputee sockets, shoe sensors, wearable sensors, wheelchair seating-system sensors, hospital-bed monitoring sensors and other ergonomics sensors.

2. Concept

The development of the optical fiber 2-D pressure sensing pad takes advantage of the highly sensitive 1-D FBG-based array structures, which are arranged in foils as shown in Fig. 1(a) to form a 2-dimensional sensing surface. The foiled optical fiber sensor elements are embedded in a thin silicon polymer material to form an elastic sensing sheet. Based on the intensity modulation caused Bragg wavelength shifting, induced by the bending of the embedded fibers, a map of displacement or force over an area is generated. The pressure is obtained from the force applied on each sensing point divided by its effective area. Multiplexed FBG array configurations are used to address applications that require multipoint monitoring of the applied external forces, where every respective FBG element comprises a single point of measurement. As shown in Fig. 1(a), longitudinal spacing d of the FBGs defines the axial spatial resolution of the linear sensor.

The 2D surface sensing is obtained by proper arrangement of FBG arrays in 2D structures, as shown in Fig. 1(a), built on a flexible and stretchable silicon-polymer Polydimethylsiloxane (PDMS) sheet. PDMS is suitable for sensing applications to match ideal skin behavior, since it is flexible, stretchable / elastic and with controllable viscosity and hardness. This pad can be wrapped around, embedded in, attached and anchored to irregularly shaped and/or moving objects or bodies and allows quasi-distributed sensing of mechanical quantities such as deformation, pressure, stress or strain along the entire surface. 2D spatial resolution is now defined by the fiber axial sensor distribution d and the spacing of optical fibers D . The presented 2D pressure sensor concept may be arranged as a uniform large scale surface [Fig. 1(a)], or may be implemented as an assembly of small scale building blocks that are properly interconnected, as shown Fig. 1(b). The second approach gives the advantage of increased sensor shape flexibility while decreasing manufacturing complexity, that comes however at the expense of increased connectorisation and surface sensing discontinuities. In the present communication, we report on the implementation and evaluation of a $2 \times 2 \text{ cm}^2$ sensing surface serving a building block for larger scale sensors.

WDM interrogation method allows for multiplexed sensor networks as each is assigned a given “slice” of the input broad-band light spectrum. We make use of a novel interrogation unit [16] [Fig. 2(a)] that features miniaturized properties, such as a weight of 150g, power consumption of <0.25 W and physical dimensions in the order of cm ($L \times W \times D$; 7x4.6x1.8 cm) while exhibiting a maximum operational frequency of 2.5 kHz for both wavelength shift and FBG central wavelength power loss measurements, an operational dynamic range of 32nm with 5pm resolution, to highlight the potential of implementing a fully portable highly sensitive sensing system.

3. Experimental Setup

A fundamental four element (2x2) FBG-based sensing surface of Fig. 1(b) is implemented by intersecting 2 rows of optical fiber patchcords, each bearing an array of 2 FBG acrylate coated sensors. The length of each FBG sensing element is 5mm and their longitudinal spacing d is fixed to 5mm, while optical fibers are spaced $D = 1$ cm, leading to a total sensing area of 2×2 cm². The optical fiber sensors are embedded in the PDMS material with a nominal elasticity of $E = 650$ kPa (Young’s Modulus) so as to produce an elastic sheet of 2.5mm thickness exhibiting a maximum allowable bend radius of 20mm. When optical fibers are embedded into the elastic PDMS material, the effective material properties of the fiber reinforced composite (i.e. homogenized average properties which can be measured experimentally) can be assumed to be linear anisotropic if deformation is small and both materials are within the linear region. Full characterization of the effective material properties of the heterogeneous composite structure can be addressed using a series of static FEA solutions [17].

For the fabrication of the sensing pad we used acrylic sheets with etched molds and holders for the optical fibers, as shown in Fig. 2(a). A CO laser system (laser beam μ m) was used to etch 250 μ m depth fiber trenches on 2.5-mm-thick acrylic boards. The optical fibers were assembled on the acrylic top board to create the composite optical FBG sensor. Then a PDMS elastomer (RTV 615 silicone elastomer made by Momentive) mixture was prepared by mixing the copolymer with a curing agent (10:1 ratio). The produced PDMS was poured into the mold, and the composite was placed in vacuum for 24 h to remove any air bubbles that have formed during mixing, until the PDMS sheet with the embedded FBG sensors was completely cured. The PDMS-based sensing pad was finally lifted away from the acrylate board after it was cured. The optical part of the experimental setup is depicted in Fig. 2(b). A Superluminescent-LED source was used to power the FBG elements of the sensing pad, while an optical coupler fed the back-reflected light to the Ibsen I-MON 80 D interrogation unit. A NI DAC card installed in a PC was used to read the extracted data.

In order to evaluate the sensor performance, a series of vertical load tests were conducted throughout the total surface of the pad sensor using a gauge test stage. A Material Tester system, the MTS 858 Mini Bionix II, was used to apply vertical force and displacement to the prototype sensor through a force gauge with a pin-head of 1cm² [Fig. 2(a)] and a universal motion controller. The resolution of the applied displacement stage was 1 μ m with a force gauge resolution of 10 mN.

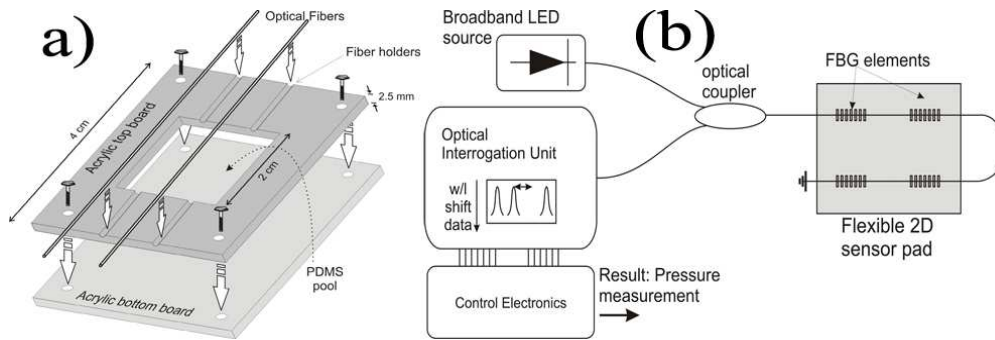


Fig. 2. a) Schematic description of the fabrication procedure for the 2x2 FBG element sensor b) experimental setup of the optical circuitry

4. Results

Figure 3(a) shows the power spectrum for all four FBGs before (blue line) and after (red line) a load was applied to FBG 3. In the blue spectrum, each peak represents the corresponding centre (Bragg) wavelength of each FBG element (4 in total) when no forces are applied. The FBG wavelengths are spaced 2nm apart, while the total wavelength range of the 2x2 sensing pad is 8nm as shown in Fig. 3(a). Each Bragg wavelength peak represents a single pressure monitoring point exhibiting a FWHM bandwidth of 0.5 nm with sidelobe suppression greater than 17dB. When vertical force or displacement is applied to a FBG element, its Bragg wavelength is shifted. In our experiment the sensor was placed on a metal table with stable temperature, to isolate the sensor from temperature variations. Temperature independent operation can be also obtained by employing an additional FBG sensor that will be responsible solely for temperature sensing without being affected by pressure. More specifically, as the proposed 2x2 pressure sensor is intended for Human-Machine interface systems in biomedical applications, sensor temperature variations will result to roughly the same wavelength shift to all FBGs. This common wavelength shift can be perceived as an offset to the pressure induced resonance shifting, which in turn can be quantified by means of the additional FBG sensor that should be located outside the pressing area acting as the temperature reference sensor. Once this offset has been quantified, sensing pad temperature calibration can then be obtained by removing this offset from the pressure-induced wavelength shift measurements.

The red spectrum of Fig. 3(a) depicts the power spectrum of the four FBG sensor elements when 400 μ m of vertical displacement corresponding to 5N force was applied to FBG3. As shown, the force applied to FBG3 produced a shift of 0.4 nm to the central wavelength of FBG3 while small variations in the FBG 2 and 4 spectrums are due to the crosstalk between the 2nm spaced FBG channels and their sidelobes overlapping.

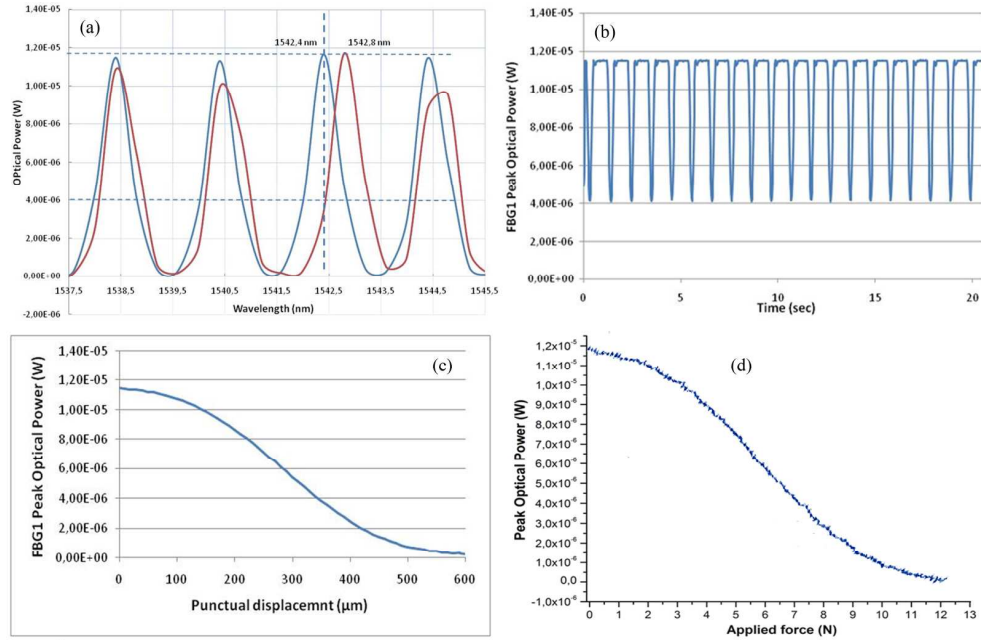


Fig. 3. Power spectrum for the 4-FBG sensor: blue line: without any axial load, red line: vertical displacement applied to FBG3. A wavelength shift occurs **b**) Power loss trace for FBG1 for 400 μm vibrating displacement applied **c**) Power loss vs vertical displacement for FBG1 (Ramp measurement) **d**) Power loss vs applied force for FBG1

The wavelength shift of FBG3 corresponds to $5.188 \times 10^{-3} \text{ MPa}^{-1}$ fractional pressure sensitivity. From the same graph, a power-loss of more than 60% was measured for the central wavelength of FBG3 corresponding to a power loss fractional pressure sensitivity of 12 MPa^{-1} . The power-loss method significantly increases the sensor sensitivity due to the autocorrelation function between the FBG filter envelope and the detection filter of the interrogator CCD pixel. However, increased sensitivity comes at the cost of restricted dynamic range, limiting the wavelength shifting tolerance of our method to the FWHM of the FBG power spectrum. A conventional wavelength shift measurement method may be applied for larger pressure values that correspond to increased wavelength shifts.

In order to further evaluate the sensitivity of the PDMS-embedded FBG sensors by means of power loss monitoring, we conducted vertical load tests for each FBG element using a 1 cm^2 head pin. The vibrating pin applied a vertical maximum displacement of $400 \mu\text{m}$ to FBG1 at 10Hz, corresponding to 5N force or 50 KPa of pressure.

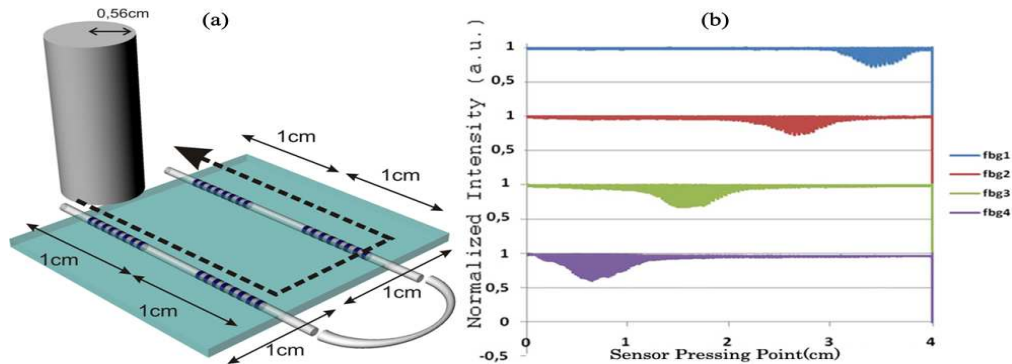


Fig. 4. a) Schematic of 2x2 sensor and sliding under the pin b) Simultaneous measurement of 4 FBG normalized intensities vs the position of the pin.

Figure 3(b) shows the optical power measurements versus time for FBG1 Bragg wavelength obtained by means of an optical photodiode. Power loss sensitivity of 60% is confirmed for every duty cycle of the vibrating pin. A short damped oscillation of the optical power appears at the end of every wave cycle on the graph. Due to its adhesive and viscoelastic characteristics, the PDMS is locally pulled upwards by the pin beyond the PDMS surface level whenever (i.e. every 1 sec) the pin returns to its starting position. When the PDMS detaches from the pin, it returns to its resting position through a damped oscillation. The oscillation translates into stress oscillation of the corresponding FBG and eventually appears as an optical power oscillation at the end of every cycle of the graph shown in Fig. 3(b). Ramp measurements with step increment of vertical displacement were also performed to identify the FBG sensors' dynamic range using the power loss method. Figure 3(c) depicts the Bragg wavelength peak power of FBG1 versus displacement and the corresponding force [Fig. 3(d)]. Step increment of displacement was set to 10 μm with overall ramp duration of 1sec. Figures 3(c), 3(d) reveal a dynamic range of 600 μm displacement, 10 N of force or 100kPa of pressure and a near-linear sensitivity of 10% power loss per 1N (10 kPa). Similar results were obtained for each of the four FBG elements.

Sensing elements for distributed pressure sensing systems have to operate independently. In particular, 1:1 mapping of each pressure reading to the corresponding point under pressure, will avoid complex mathematical post-processing of the results. To verify the independent operation of each FBG sensing element in our configuration, we slid the 2x2 fiber optic sensing pad in a circular manner under a vibrating pin with 1 cm^2 -rounded head, as shown in Fig. 4(a). The pin vibrated at a frequency of 10 Hz and a peak-to-peak vertical displacement of 250 μm . We simultaneously measured the peak power of each FBG Bragg wavelength and the result is depicted in Fig. 4(b). The horizontal axis of Fig. 4(b) refers to the relative pressing point in cm as the pin moves over the FBGs, while normalized intensity values are used for the FBG Bragg wavelengths to compensate for the different mean optical powers between the two fiber optic patch-cords. The result clearly shows independent operation of each FBG sensor within the 1cm fiber axial length, while the spatial resolution of the FBG sensing elements is calculated to as low as 1 cm^2 .

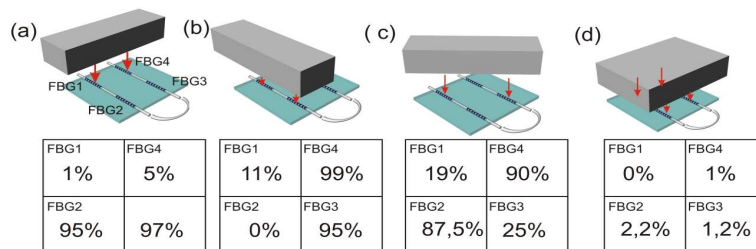


Fig. 5. : a-d) Multipoint operation of 2D sensor, with the tables of corresponding power loss.

In order to study the fiber-based sensor operation under more realistic conditions, we tested the sensor in multipoint operation using a rectangular metal bar with 1cm edge to press all possible 2-point combinations and a metal plate with a surface larger than the total sensor to press all four sensing points. The metal patterns were set to vibrate at a frequency of 10 Hz and for a peak-to-peak displacement of 600 μm , driving the sensing elements to their operational limits. Figure 5(a), 5(b), 5(c), 5(d) depict some of these cases along with the tables indicating the percentage of optical power received for each FBG wavelength at the moment of maximum displacement. In Fig. 5(a), 5(b), 5(d), small variations in the indicated FBG power losses are due to the slightly different response of each FBG. Figure 5(c) shows that aside from FBGs 1 and 3, small power losses occur in FBGs 2 and 4 due to unwanted partial overlapping between the 1cm metal bar and the latter FBGs. However, clear identification of the multipoint pattern is still allowed. Finally, it should be noted that while the fiber deformation mechanism for the pin-based experiments relies on fiber bending, in Fig. 5(d) the

axial extension of the FBGs is due to the Poisson effect material expansion of the PDMS that exhibits a Poisson ratio nominal value of 0.5.

5. Conclusion

We have presented a novel optical fiber based 2D pressure sensor exhibiting a high sensitivity of 10% optical power loss per 10kPa pressure and a high spatial resolution of 1cm². The sensing elements have a real-time response and demonstrated no hysteresis, while their operation is independent, yielding a 1:1 correlation of each FBG sensor indication to the respective sensing point without the need of data post-processing and allowing for easy pressure pattern identification in multi-point operation. The presented 2x2 cm² sensing surface is easily expandable and can be used as a building block for larger scale sensors. The mechanical properties of the presented sensor pad allow for embedding or attaching the sensor to irregular shapes and geometries, offering enhanced response to curvature while the low physical dimension commercially available interrogation unit enhances the portability features of the complete sensing system. The sensor's minimal thickness, make it very unobtrusive, with minimal interference on the measurement interface. These attractive physical and operational characteristics are ideally suited for biomedical applications in biomechanics, rehabilitation and orthotics such as amputee sockets, shoe sensors, wearable sensors and wheelchair/hospital bed -system sensors.

Acknowledgments

EU-FP7-SME-2008-1 Intelligent Adaptable Surface with Optical Fiber Sensing for Pressure-Tension Relief – IASiS, U.S. ARMY MEDICAL RESEARCH & MATERIEL COMMAND, “MOVE” CENTER Award: # 07-2-01, and IBSEN Photonics LLC., for providing the miniaturized IMON-80-D interrogation unit.